Available online at www.sciencedirect.com

SciVerse ScienceDirect

Ceramics International 38 (2012) 2455–2459

CERAMICS INTERNATIONAL

www.elsevier.com/locate/ceramint

Synthesis and structural properties of cubic G0-$Rb_2KMoO_3F_3$ oxyfluoride

V.V. Atuchin [a,*], T.A. Gavrilova [b], L.I. Isaenko [c], V.G. Kesler [d], M.S. Molokeev [e], S.A. Zhurkov [c]

[a] Laboratory of Optical Materials and Structures, Institute of Semiconductor Physics, SB RAS, Novosibirsk 90, 630090, Russia
[b] Laboratory of Nanolithography and Nanodiagnostics, Institute of Semiconductor Physics, SB RAS, Novosibirsk 90, 630090, Russia
[c] Laboratory of Crystal Growth, Institute of Geology and Mineralogy, SB RAS, Novosibirsk 90, 530090, Russia
[d] Laboratory of Physical Principles for Integrated Microelectronics, Institute of Semiconductor Physics, SB RAS, Novosibirsk 90, 630090, Russia
[e] Laboratory of Crystal Physics, Institute of Physics, SB RAS, Krasnoyarsk 36, 660036, Russia

Received 23 September 2011; received in revised form 24 October 2011; accepted 4 November 2011
Available online 10 November 2011

Abstract

High-temperature G0 polymorph of $Rb_2KMoO_3F_3$ has been prepared by melt solidification. Micromorphology and chemical properties of the final product were evaluated by scanning electron microscopy (SEM) and X-ray photoelectron spectroscopy (XPS). The elpasolite-related crystal structure of G0-$Rb_2KMoO_3F_3$ has been refined by Rietveld method at $T = 298$ K (space group $Fm\text{-}3m$, $a = 8.92446(8)$ Å, $V = 710.76(1)$ Å^3; $R_B = 3.55\%$). Ferroelectric G1-$Rb_2KMoO_3F_3$ polymorph, earlier reported at $T < 328$ K, is not found at $T = 298$ K.

Keywords: A. Powders: solid state reaction; B. Microstructure-final; B. X-ray methods; D. Alkali oxides; D. Halides

1. Introduction

Rubidium potassium oxyfluoromolybdate, $Rb_2KMoO_3F_3$, is a member of wide oxyfluoride family $A_2BMO_3F_3$ (A, B = Na, K, Rb, Cs, Tl, NH_4, Ag; M = Mo, W) with elpasolite-related crystal structure [1–8]. Generally, compounds $A_2BMO_3F_3$ (A, B = Na, K, Rb, Cs, Tl, NH_4, Ag) exhibit a sequence of reciprocal phase transitions on temperature decrease [2–5,9,10]. As it is stated in several structural studies, the transitions are related to partial ordering of O/F atoms in anion positions. In the low-temperature states Gi ($i > 0$) many oxyfluorides from $A_2BMO_3F_3$ family are found to be noncentrosymmetric and possess the ferroelectric properties [2–5,7,9–12]. Complete O/F disorder in the anion positions, however, is found for high temperature cubic G0-phase with space group $Fm\text{-}3m$ [5,10,11,13–15]. Also, the structural transitions on temperature variation are known for many other oxyfluorides with anion content O/F ≠ 3 and this is an indicator of the thing that the characteristic temperature of structural transition may be strongly dependent on the real chemical composition of oxyfluoride crystal, in particular the O/F ratio.

As it was obtained, cubic phase G0-$Rb_2KMoO_3F_3$ exists above temperature $T > 328$ K, and two phases with ferroelectric properties were observed at $T < 328$ K [3]. The crystalline materials with phase transitions few above ambient temperature are of special interest for several applications and the detailed observation of crystal properties is actual for such compounds. Earlier, the $Rb_2KMoO_3F_3$ was synthesized by solid state reaction between alkali metal fluorides and MoO_3 at $T = 873$ K in argon atmosphere [1,3]. A single crystal growth of G0-$Rb_2KMoO_3F_3$ by Bridgman technique was also reported [13]. In these both studies, however, there was no detailed description of the technological conditions used for the crystal synthesis. Commonly, the polarity of $MoO_{6-x}F_x$ octahedron is strongly dependent on O/F ratio with maximum at O/F = 3 [16,17]. Respectively, to have reproducible results on phase composition and physical properties of an oxyfluoride, the technology should be stabilized with respect to fluoride component loss during synthesis. It should be also accounted that the appearance of Mo^{4+} and Mo^{5+} ions is possible due to incomplete oxidation of molybdenum atoms in nonstoichiometric oxyfluoromolybdates possessing noticeable electrical conductivity [18]. Thus, the present study is aimed at the design of technology for the stable synthesis of G0-$Rb_2KMoO_3F_3$ compound and the observation of structural and morphological properties of the final product.

* Corresponding author. Tel.: +7 383 3308889; fax: +7 383 3332771.
E-mail address: atuchin@thermo.isp.nsc.ru (V.V. Atuchin).

0272-8842/$36.00
doi:10.1016/j.ceramint.2011.11.013

2. Experimental

The $Rb_2KMoO_3F_3$ compound was formed by solid state synthesis in accordance with the earlier proposed reaction [1,3]:

$$2RbF + KF + MoO_3 = Rb_2KMoO_3F_3.$$

High purity initial reagents $KF{\cdot}2H_2O$, Rb_2CO_3, MoO_3, NH_4F (all 99.9%, CJSC ''Plant of rare metals'', Russia) and aqueous hydrofluoric acid (HF) (48% HF by weight, CJSC ''Plant of rare metals'', Russia) were used. To avoid the drastic capture of air agents into KF and RbF reagents, all the reactions and heat treatments were produced under dried nitrogen atmosphere at increased pressure. KF was synthesized by vaporization of a mixture of $KF{\cdot}2H_2O$ and hydrofluoric acid. Then, the NH_4F was added to KF powder and the mixture was heated up to $T = 573$ K into the closed Teflon crucible to remove the residual OH-groups (KOH species) in accordance with the reaction:

$$KOH + NH_4F = KF + H_2O\uparrow + NH_3\uparrow.$$

Then, to create the pure dry KF the fluorine-agent CF_4 was added into the powder and the mixture was placed into a closed platinum crucible and heated to $T = 773$ K. Then, the cooled KF powder was grinded, placed into the open platinum crucible and heated to $T = 1173$ K, that is far above KF melting temperature, under dried nitrogen flow for the time $t = 3$ h and cooled to room temperature at the rate 50 K/h. RbF was synthesized by the reaction of Rb_2CO_3 with excess hydrofluoric acid followed by vaporization up to solid powder. Then, dry RbF was fabricated by the same procedures as those used for KF, but the final melt treatment was produced at lower temperature $T = 1073$ K. Owing to their hygroscopic nature, the alkali fluoride products were kept and manipulated under dried nitrogen into a glove box. The starting mixture of KF, RbF and MoO_3 was prepared in stoichiometric composition ratio related to $Rb_2KMoO_3F_3$ nominal. The mixture was grinded, placed into the open platinum crucible and heated to $T = 1073$ K at the rate of 100 K/h. Then, the melt was being cooled to room temperature together with furnace for $t = 24$ h. The final product of the reaction in the melt was a dense uniform milk color disk-like agglomerate of ~35 mm in diameter and ~10 mm in thickness.

The micromorphology of the product was evaluated with scanning electron microscopy (SEM) using LEO 1430 device. Chemical composition and molybdenum valence state were defined by X-ray photoelectron spectroscopy (XPS) method using the surface analysis center SSC (Riber). To prepare the sample for XPS measurements, a fragment of $Rb_2KMoO_3F_3$ was grinded up to powder state and pressed into a freshly prepared indium foil. The nonmonochromatic Al Kα radiation (1486.6 eV) with the power source of 300 W was used for the excitation of photoemission. The measurement conditions and energy scale calibration method can be found elsewhere [19,20]. A pronounced drift of energy scale, due to charging effects, was detected because of the dielectric nature of $Rb_2KMoO_3F_3$ surface. This drift was taken into account with reference to the position of C 1s (284.6 eV) line generated by adventitious carbon on the surface of powder as-inserted into vacuum chamber.

The powder X-ray diffraction pattern for Rietveld analysis was collected at room temperature (298 K) with a Bruker D8 ADVANCE diffractometer in the Bragg-Brentano geometry and linear Vantec detector. The operating parameters were: Cu Kα radiation, tube voltage 40 kV, tube current 40 mA, step size 0.016°, counting time 1 s per step. The data were collected over 2θ range 5–110°. The peak positions were determined with the program EVA available in the PC software package DIFFRAC-PLUS supplied from Bruker.

3. Results and discussion

SEM images of $Rb_2KMoO_3F_3$ surface are shown in Fig. 1. To see the internal morphology, the bulk agglomerate was cracked mechanically and the fragment surfaces were evaluated by SEM. As it is evident from the image shown in Fig. 1, the surface is hilly and without noticeable crystal facets. The uniform gray contrast in these SEM images indicates the chemical uniformity of the sample. Dark sports visible in Fig. 1a are the pores appeared, as it seems, due to bulk material

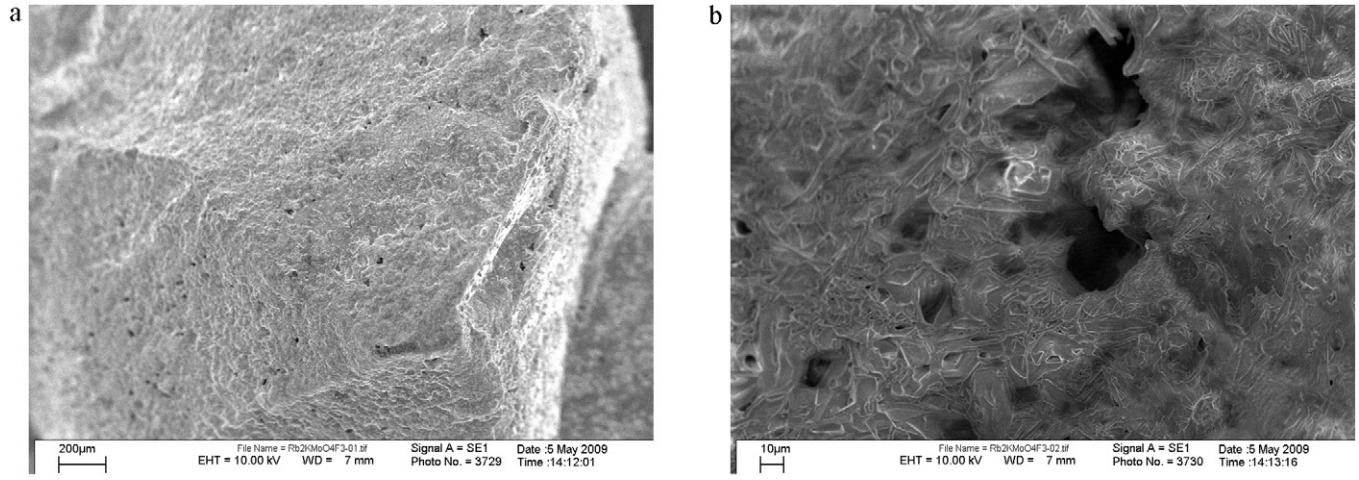

Fig. 1. SEM images of (a) cracked surface and (b) a pore of G0-$Rb_2KMoO_3F_3$ fragment.

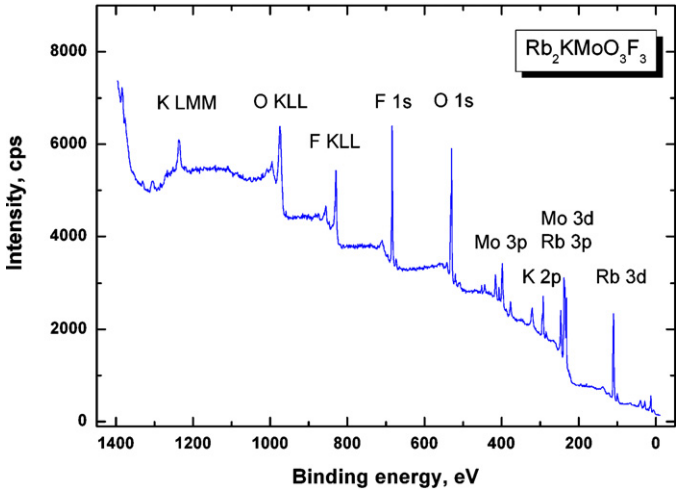

Fig. 2. Survey photoemission spectrum from G0-$Rb_2KMoO_3F_3$.

shrinkage on cooling after solidification. One such pore is shown in Fig. 1b. Interesting formations were found in the central part of external surface of the disk formed after melt solidification. An example of such formations is shown in Fig. S1. This part of the disk agglomerate was not contacting the walls of the platinum crucible. The regular rectangular spots were detected at the surface of the formations. As it seems, these square-like spots appeared due to cubic $Rb_2KMoO_3F_3$ crystals growing in the disk bulk.

The survey photoemission spectrum is shown in Fig. 2. Besides spectral features related to constituent element core levels and Auger lines, the weak signal of C 1s core level was found in the spectrum. The C 1s line is apparently due to the presence of hydrocarbons captured at the sample surface from the air. In Fig. 3 the Mo 3d doublet recorded by XPS is shown. It is well known that the binding energy (BE) of Mo $3d_{5/2}$ and Mo $3d_{3/2}$ components is strongly dependent on the molybdenum ion valence state in oxides [18,21]. In $Rb_2KMoO_3F_3$ the Mo 3d doublet is partly crossing the Rb 3p doublet and an accurate

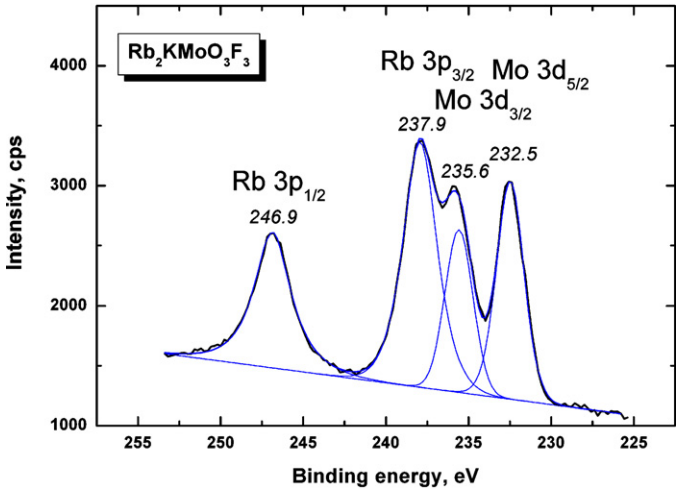

Fig. 3. Detailed spectrum of Mo 3d and Rb 3p doublets from G0-$Rb_2KMoO_3F_3$.

Table 1
Constituent element ratio in the synthesized sample.

Element (core level)	Rb (Rb 3d)	K (K $3p_{3/2}$)	Mo (Mo $3d_{5/2}$)	O (O 1s)	F (F 1s)
Sample	0.21	0.10	0.09	0.35	0.25
$Rb_2KMoO_3F_3$, nominal	0.20	0.10	0.10	0.30	0.30

peak fitting procedure was implemented to reveal the shape and BE position of Mo $3d_{5/2}$ and Mo $3d_{3/2}$ components. The Mo $3d_{5/2}$ and Mo $3d_{3/2}$ components are narrow and symmetrical. The BE values defined for the Mo $3d_{5/2}$ and Mo $3d_{3/2}$ components by fitting analysis are shown in Fig. 3. These values are well related to the BE values typical of Mo^{6+} ions in oxides [21,22]. The chemical composition of $Rb_2KMoO_3F_3$ sample was estimated with XPS using the Rb 3d, K $3p_{3/2}$, Mo $3d_{5/2}$, O 1s and F 1s lines and tabulated data on the atomic sensitivity factors (ASF) [21]. The results of calculations are shown in Table 1. The constituent element ratio estimated by XPS is well related to that of stoichiometric $Rb_2KMoO_3F_3$.

Fig. 4 shows the XRD curve recorded for the powder sample of $Rb_2KMoO_3F_3$. Only few peaks of very weak intensity and related to foreign phases were revealed in the XRD pattern. The structure of G0-phase of $Rb_2KMoO_3F_3$ is isostructural to elpasolite (sp. gr. *Fm-3m*), so we use these coordinates of atoms to refine the structure of $Rb_2KMoO_3F_3$. All refinements and data processing were performed by DDM program [23]. The Pearson VII function was used to model the peak profiles. The refinement of the structure with *Fm-3m* space group was stable and it led to minimal *R*-factor (Table 2). The coordinates of atoms, isotropic thermal parameters and occupations of atom positions are given in Table 3. Experimental (dots) and theoretical (lines) X-ray diffraction patterns of G0-$Rb_2KMoO_3F_3$ are shown in Fig. 4. The main bond lengths are reported in Table 4. The crystal structure of G0-$Rb_2KMoO_3F_3$ is shown in Fig. 5 and it can be considered as a sequence of corner-linked $Mo(O,F)_6$ and $K(O,F)_6$ octahedra.

It is interesting to compare the cell parameter value obtained for G0-$Rb_2KMoO_3F_3$ in Ref. [13] to that defined in the present study. The value $a = 8.945(5)$ Å specified for single crystal sample of G0-$Rb_2KMoO_3F_3$ at $T = 343$ K is noticeably higher than the value $a = 8.92446(8)$ Å found in the present study at

Table 2
The main parameters of crystal structure processing and refinement.

Space group	*Fm-3m*
a (Å)	8.92446(8)
V (Å^3)	710.76(1)
2θ-interval range (°)	5–110
Number of reflexions	39
Number of refinement parameters	8
R_B (%)	3.55
R_{DDM} (%)	10.97

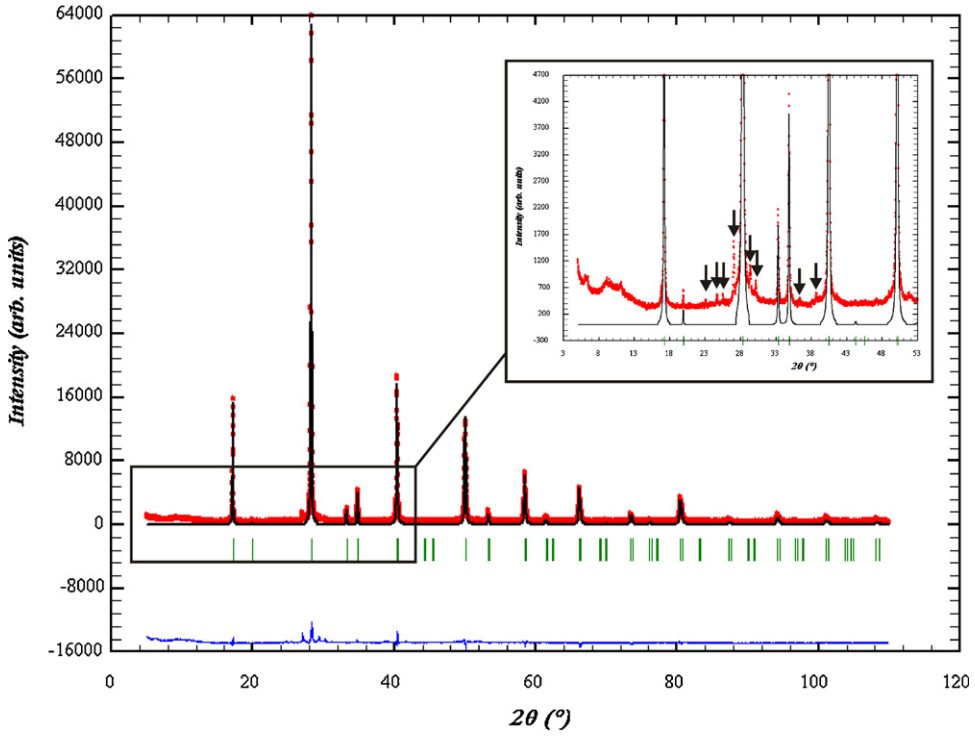

Fig. 4. Experimental (dots) and theoretical (lines) X-ray diffraction patterns of G0-$Rb_2KMoO_3F_3$ at $T = 298$ K. Peaks of alien phases are marked by arrows.

Table 3
Coordinates of atoms, isotropic thermal parameters (B_{iso}) and occupation of atom positions (p) of structure $Rb_2KMoO_3F_3$ at room temperature.

Atom	p	X	Y	Z	$B_{iso.}$ (Å^2); U_{ij} (Å^2)
Rb	1.0	1/4	1/4	1/4	4.04(5)
Mo	1.0	0	0	0	3.72(5)
K	1.0	1/2	1/2	1/2	1.9(1)
F	0.5	0.2119(5)	0	0	$U_{11} = U_{22} = 0.0144(5)$; $U_{33} = 0.0085(9)$
O	0.5	0.2119(5)	0	0	$U_{11} = U_{22} = 0.0144(5)$; $U_{33} = 0.0085(9)$

$T = 298$ K. This drastic disparity, however, seems be related to a difference in the temperature of measurements. Earlier, a strong dependence of the cell parameter on temperature in cubic G0-$Rb_2KMoO_3F_3$ was specified over the range $T = 343$–473 K [13]. If to extrapolate the $a(T)$ curve down to $T = 298$ K, one can calculate the value $a \sim 8.928$ Å accounting for a possible error in $a(T)$ curve determination. This value is in a reasonable relation with that obtained in our experiment. So, it may be concluded that the temperature range of existence of cubic modification G0-$Rb_2KMoO_3F_3$ can be expanded up to $T = 298$ K.

Table 4
The main interatomic distances in structure $Rb_2KMoO_3F_3$ at room temperature.

Bond	Length (Å)
Mo–O(F)	1.891(5)
Rb–O(F)	3.174(5)
K–O(F)	2.571(5)

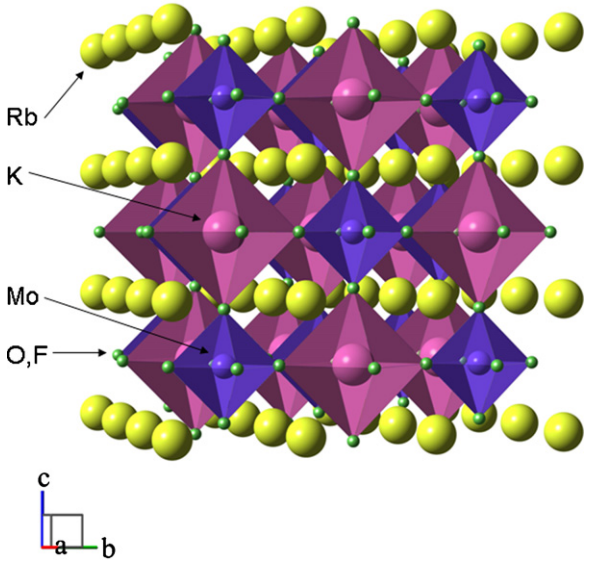

Fig. 5. Crystal structure of G0-$Rb_2KMoO_3F_3$ at $T = 298$ K.

4. Conclusions

The $Rb_2KMoO_3F_3$ oxyfluoromolybdate is prepared by accurate solid state synthesis. However, ferroelectric G1-$Rb_2KMoO_3F_3$ phase which existence was earlier reported over the range $T < 328$ K is not found by our measurements. At $T = 298$ K the cubic G0-$Rb_2KMoO_3F_3$ was found by crystal structure analysis of our polycrystalline sample. Respectively, the temperature of the phase transition G0 ↔ G1 should be shifted at least to the range $T < 298$ K, if the transition ever occurs.

Acknowledgments

This study was partly supported by RFBR (Grant 09-02-00062) and SB RAS (Grant 34).

Appendix A. Supplementary data

Supplementary data associated with this article can be found, in the online version, at doi:10.1016/j.ceramint.2011.11.013.

References

[1] G. Pausewang, W. Rüdorff, $A_3^{I}MeO_xF_{6-x}$-Verbindungen mit $x = 1, 2, 3$, Z. Anorg. Allg. Chem. 364 (1969) 69–87.
[2] G. Péraudeau, J. Ravez, A. Tressaud, P. Hagenmuller, H. Arend, G. Chanussot, Les transitions de phase de l'oxyfluorure $Rb_3MoO_3F_3$, Solid State Commun. 23 (1977) 543–546.
[3] G. Péraudeau, J. Ravez, H. Arend, Etude des transitions de phases des composes $Rb_2KMO_3F_3$, $Cs_2KMO_3F_3$ et $Cs_2RbMO_3F_3$ (M = Mo, W), Solid State Commun. 27 (1978) 515–518.
[4] F.J. Brink, L. Norén, R.L. Withers, Synthesis, electron diffraction, XRD and DSC study of the new elpasolite-related oxyfluoride, $Tl_3MoO_3F_3$, J. Solid State Chem. 174 (2003) 44–51.
[5] I.N. Flerov, M.V. Gorev, V.D. Fokina, M.S. Molokeev, Phase transitions in oxides, fluorides and oxyfluorides with the ordered perovskite structure, Ferroelectrics 346 (2007) 77–83.
[6] W. Tong, W.-S. Yoon, N.M. Hagh, G.G. Amatucci, A novel silver molybdenum oxyfluoride perovskite as a cathode material for lithium batteries, Chem. Mater. 21 (2009) 2139–2148.
[7] V.V. Atuchin, T.A. Gavrilova, V.G. Kesler, M.S. Molokeev, K.S. Aleksandrov, Low-temperature synthesis and structural properties of ferroelectric $K_2WO_3F_3$ elpasolite, Chem. Phys. Lett. 493 (2010) 83–86.
[8] J.M. Chamberlain, T.A. Albrecht, J. Lesage, F. Sauvage, C.L. Stern, K.R. Poeppelmeier, Crystal growth of $Ag_3MO_xF_{6-x}$ (M = V, $x = 2$; M = Mo, $x = 3$), Crystal Growth Des. (2010), doi:10.1021/cg100890e.
[9] G. Peraudeau, J. Ravez, P. Hagenmuller, H. Arend, Study of phase transitions in $A_3MO_3F_3$ compounds (A = K, Rb; Cs; M = Mo, W), Solid State Commun. 27 (1978) 591–593.
[10] I.N. Flerov, V.D. Fokina, A.F. Bovina, E.V. Bogdanov, M.S. Molokeev, A.G. Kocharova, E.I. Pogorel'tsev, N.M. Laptash, Mechanism and nature of phase transitions in the $(NH_4)_3MoO_3F_3$ oxyfluoride, Phys. Solid State 50 (3) (2008) 515–524.
[11] J.-P. Chaminade, M. Cervera-Marzal, J. Ravez, P. Hagenmuller, Ferroelastic and ferroelectric behavior of the oxyfluoride $Na_3MoO_3F_3$, Mater. Res. Bull. 21 (1986) 1209–1214.
[12] Z.G. Ye, J. Ravez, J.-P. Rivera, J.-P. Chaminade, H. Schmid, Optical and dielectric studies on ferroelectric oxyfluoride $K_3MoO_3F_3$ single crystals, Ferroelectrics 124 (1991) 281–286.
[13] S.C. Abrahams, J.L. Bernstein, J. Ravez, Paraelectric–paraelastic $Rb_2KMoO_3F_3$ structure at 343 and 473 K, Acta Crystallogr. B 37 (7) (1981) 1332–1336.
[14] M.S. Molokeev, A.D. Vasiliev, A.G. Kocharova, Crystal structures of room- and low-temperature phases in oxyfluoride $(NH_4)_2KWO_3F_3$, Powder Diffr. 22 (3) (2007) 227–230.
[15] A.A. Udovenko, N.M. Laptash, Orientational disorder in crystals of $(NH_4)_3MoO_3F_3$ and $(NH_4)_3WO_3F_3$, Acta Crystallogr. B 64 (3) (2008) 305–311.
[16] P.A. Maggard, T.S. Nault, C.L. Stern, K.R. Poeppelmeier, Alignment of acentric $MoO_3F_3^{3-}$ anions in a polar material: $(Ag_3MoO_3F_3)(Ag_3MoO_4)Cl$, J. Solid State Chem. 175 (2003) 27–33.
[17] R.L. Withers, F.J. Brink, Y. Liu, L. Norén, Cluster chemistry in the solid state: structured diffuse scattering, oxide/fluorine ordering and polar behaviour in transition metal oxyfluorides, Polyhedron 26 (2007) 290–299.
[18] N.M. Laptash, Y.M. Nikolenko, N.M. Mishchenko, Mixed valence in nonstoichiometric molybdenum oxyfluorides, Z. Neorg. Khim. 42 (5) (1997) 765–768.
[19] V.V. Atuchin, T.A. Gavrilova, J.-C. Grivel, V.G. Kesler, Electronic structure of layered titanate $Nd_2Ti_2O_7$, Surf. Sci. 602 (2008) 3095–3099.
[20] V.V. Atuchin, T.A. Gavrilova, V.G. Kesler, M.S. Molokeev, K.S. Aleksandrov, Structural and electronic parameters of ferroelectric $K_3WO_3F_3$, Solid State Commun. 150 (2010) 2085–2088.
[21] C.D. Wagner, W.M. Riggs, L.E. Davis, J.F. Moulder, G.E. Muilenberg (Eds.), Handbook of X-ray Photoelectron Spectroscopy, Perkin-Elmer Corp., Phys. Elect. Div., Minnesota, 1979.
[22] C.V. Ramana, V.V. Atuchin, V.G. Kesler, V.A. Kochubey, L.D. Pokrovsky, V. Shutthanandan, U. Becker, R.C. Ewing, Growth and surface characterization of sputter-deposited molybdenum oxide thin films, Appl. Surf. Sci. 253 (12) (2007) 5368–5374.
[23] L.A. Solovyov, Full-profile refinement by derivative difference minimization, J. Appl. Crystallogr. 37 (2004) 743–749.